EUROPEAN ORGANIZATION FOR NUCLEAR RESEARCH
CERN — SL DIVISION

CERN-SL-2000-019 HRF

Study of a Single-Bunch Instability below Transition Energy

T. Bohl, T. Linnecar, E. Shaposhnikova

Abstract

In the CERN SPS microwave instability is an important limitation for the single bunch intensity of a proton beam. In the past this instability has been studied at energies above transition energy. In this paper we describe recent observations concerning the instability in the SPS at two different energies below transition. The results are compared with those obtained by the same measurement method above transition as well as with results from numerical simulations.

Paper presented at EPAC 2000, 26-30 June 2000, Vienna, Austria

Geneva, Switzerland
June 2000

Study of a Single-bunch Instability below Transition Energy

T. Bohl, T. Linnecar, E. Shaposhnikova
CERN, Geneva, Switzerland

Abstract

In the CERN SPS microwave instability is an important limitation for the single bunch intensity of a proton beam. In the past this instability has been studied at energies above transition energy. In this paper we describe recent observations concerning the instability in the SPS at two different energies below transition. The results are compared with those obtained by the same measurement method above transition as well as with results from numerical simulations.

1 INTRODUCTION

The microwave instability already became an issue in the SPS a few years after commissioning [1]. Today it is of interest both above transition energy, in view of the requirements of the beams for LHC [2], and below transition, because of the high intensity beam to be used for the CNGS, CERN Neutrinos to Gran Sasso, project [3].

First measurements below transition were done at 14 GeV/c, the injection energy for CNGS. However this paper is mainly focused on experiments below transition with $\gamma = 21.3$, and presents a comparison with previously acquired data above transition at $\gamma = 27.7$ [4]. The energy, $\gamma = 21.3$, was chosen to have approximately the same debunching time, $t_d = \tau/(2|\eta|\Delta p/p)$, at both energies. Here τ is the initial bunch length, $\eta = 1/\gamma_t^2 - 1/\gamma^2$ and $\Delta p/p$ is the momentum spread. Table 1 shows the relevant machine and beam parameters.

The experimental method used is based on the analysis of the unstable bunch spectrum developing during slow debunching [4]. The spectrum has peaks corresponding to different resonant impedances, (with high R/Q and low Q, R being the shunt impedance and Q the quality factor), and has been used to identify the dominant sources of impedance in the SPS.

A single proton bunch is injected into the SPS with all five RF systems off (passively or actively damped). The beam signals from a longitudinal wideband monitor, 4 MHz to 4 GHz, are acquired either with a digital oscilloscope, (sampling time 250 ps), or with a spectrum analyser. Bunch profiles are analysed both in time and frequency domain.

$\gamma_t = 23.2$		p = 20 GeV/c	p = 26 GeV/c
γ		21. 3	27.7
τ	ns	22	24
ε	eVs	0.2	0.24
$\Delta p/p$		$\pm 2.9 \times 10^{-4}$	$\pm 2.5 \times 10^{-4}$
η		-3.46×10^{-4}	5.53×10^{-4}
t_d	ms	110	87
$\gamma(\Delta p/p)^2\lvert\eta\rvert$		6.3×10^{-10}	9.2×10^{-10}
N_{p}		3.5×10^{10}	3.5×10^{10}

Table 1: Machine and initial beam parameters.

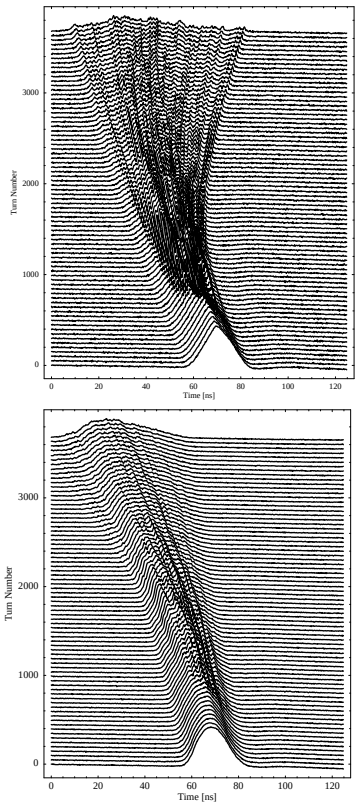

Figure 1: Mountain range in time domain for $\gamma = 21.3$ (top) and $\gamma = 27.7$ (bottom).

2 TIME DOMAIN ANALYSIS

Fig. 1 shows mountain range plots for bunches of similar intensity below and above transition. One can see that, below transition, a) the bunch is more unstable (as indicated by the bunch shape modulation at high frequencies), b) it debunches faster than above transition. The first point is in agreement with the stability criterion for both broadband [5], [6], and narrow-band impedances [7], since the threshold of the fast microwave instability is proportional to $\gamma(\Delta p/p)^2|\eta|$ (see Table 1 for numerical values). However faster debunching is in contradiction with what one would expect if no intensity effects are taken into account

or if only the effect of a reactive impedance with Im(Z/n) = $const$ is included. In the SPS, the contribution from space charge impedance is small (1-2 Ω) in comparison with the inductive wall impedance ($\geq$ 10 Ω). This would lead to a focusing (defocusing) voltage below (above) transition and thus increase (decrease) the debunching time [8].

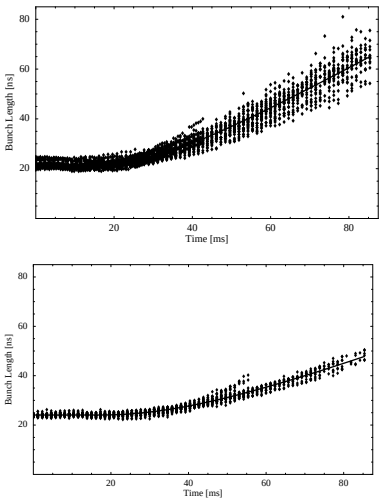

Figure 2: Bunch length during debunching, $\gamma = 21.3$ (top) and $\gamma = 27.7$ (bottom). Intensities $(2.8 - 4.3) \times 10^{10}$.

The plots of bunch length (defined as the total width of the bunch at 15% of its peak amplitude) versus time for all acquisitions, below and above transition, are presented in Fig. 2. The data shows that up to $\sim$ 20 ms the bunches hardly debunch (as would be expected from their initial parameters, see t_d in Table 1). Then the momentum spread of the unstable beam blows up resulting in a faster debunching time in both cases. From the slope of the curves in Fig. 2 it is roughly two times more rapid below transition than above. Before the effect of the instability is noticed as a change in bunch length, it is observed on the peak amplitude signal due to line density modulation, (Fig. 3, below transition).

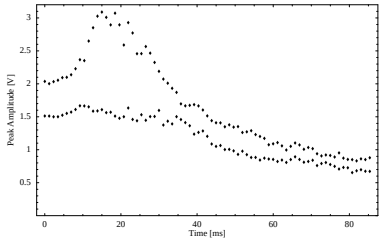

Figure 3: Bunch peak amplitude during debunching for $\gamma = 21.3$, $N_{\rm p} = 2.8 \times 10^{10}$ (bottom trace) and $N_{\rm p} = 4.3 \times 10^{10}$ (top trace).

Apart from the fact that in our experiment the bunch below transiton was more unstable and is likely therefore to have a larger momentum blow-up, faster debunching

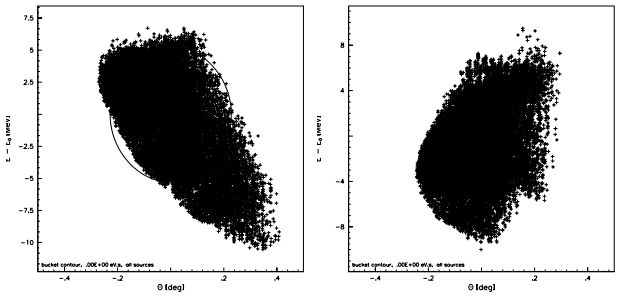

Figure 4: Phase space distribution (ESME) below (left) and above (right) transition 50 ms after injection. $|\eta| = 5.2 \times 10^{-4}$. Resonant impedance at: f_{res} = 1.6 GHz, Q = 100, R/Q = 30 kΩ. Bunch: $N = 3{\times}10^{10}$, ε = 0.24 eVs. Partially hidden curve shows initial bunch.

below transition has an additional explanation. Both in the measurements, Fig. 1, and in simulations, Fig. 4, it is seen that line density modulation grows in amplitude along the bunch from the head to the tail. The particles form micro-bunches and lose energy. In phase space, Fig. 4, these appear as "drops" below the point of formation. Off-momentum particles move in different directions above and below transition, the bunch leaning left or right in phase space. Below transition the particles falling from the tail produce an overall increase in total $\Delta p/p$. These particles will move faster and give a quicker increase in bunch length. This can already be seen in Fig. 4, where the bunch length is very different in the two cases.

Simulations with RF on, using the same parameters, show that the development of the instability is very similar at the beginning to the case with RF off. The bunch is unstable both above and below transition, compare the results in [9]. This could not be tested experimentally for long bunches, in the absence of an adequate capture system in the SPS.

3 FREQUENCY DOMAIN ANALYSIS

In Fig. 5 we present mountain range data in the frequency domain. Below transition a high frequency excitation ($\sim$ 1.5 GHz) is dominant, and at the beginning practically suppresses all other known peaks which are however well seen above transition. The peak at 1.5 GHz is due to the strongest mode in the pumping ports; there are $\sim$ 800 of these cavity-like objects in the ring. Unlike the case above transition, this excitation does not disappear at later times but moves to lower frequencies. As can be seen in time domain the excitation consists of a certain number of periods along the bunch which practically does not change with time. However as time increases these periods stretch out and the frequency progressively decreases.

When sweeping through other different resonant impedances, the amplitude of excitation grows. This effect is well seen in the contour plot, Fig. 6. Particularly interesting is that apart from known impedances, e.g. the TW cavities at 800 MHz, it also brings out some other frequencies,

around 1 GHz, which were under suspicion from coupled-bunch instability studies, and presumably have high Q.

Due to this sweep process, the mode spectrum, if defined as a projection of the mountain range data in frequency domain onto the frequency axis [4], looks quite different depending on the time the projection is made, $T_{\rm obs}$. In the case of $\gamma > \gamma_{\rm t}$, the sweep process is less marked and the spectra do not depend in the same way on $T_{\rm obs}$. Fig. 7 compares several mode amplitude spectra at different $T_{\rm obs}$. Taking into account the effect of $T_{\rm obs}$, one can see that the peaks corresponding to different impedances in the ring line up fairly well.

Measurements above 2 GHz were done with a spectrum analyser due to the restricted sampling rate of the digital oscilloscope used for bunch profile acquisition. The data (not shown here) for the two energies below transition have the same resonant structure as above transition.

4 SUMMARY

The single-bunch instability, previously observed above transition energy and used to identify different impedance sources in the SPS ring, have now also been observed below transition at a roughly equal value of $|\eta|\,\Delta p/p$. While the mode amplitude spectra below and above transition agree fairly well, the detailed bunch behaviour is however quite different. In our experiments, below transition the instability induced modulation persists longer, the debunching is faster, and the observed momentum blow-up is larger.

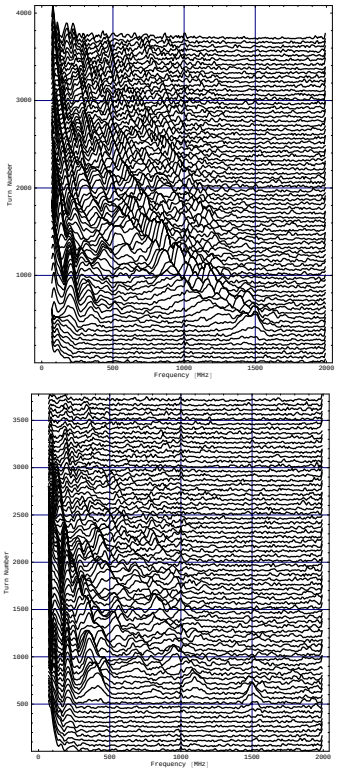

Figure 5: Mountain range in frequency domain for $\gamma = 21.3$, top, and $\gamma = 27.7$, bottom.

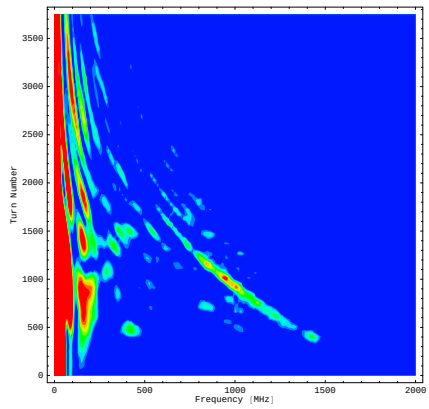

Figure 6: Contour plot of mountain range in frequency domain (blue: low amplitude, red: high amplitude).

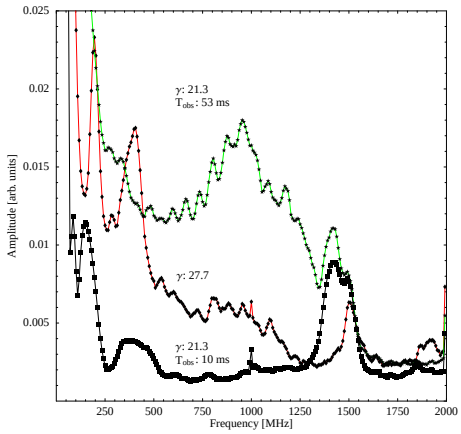

Figure 7: Mode amplitude spectra for $\gamma = 27.7$ and $\gamma = 21.3$ at different $T_{\rm obs}$. Isolated peaks at exactly 1 GHz and 2 GHz are instrumental artifacts.

The frequency sweeping process below transition gives an extra possibility to identify new impedance sources in the ring.

5 REFERENCES

[1] D. Boussard, G. Dome, T. Linnecar, A. Millich, IEEE Trans. Nucl. Sci. Vol. NS-24, No. 3, 1977, pp. 1399-1401.

[2] Ed. P. Lefevre, T. Pettersson, CERN/AC/95-05 (LHC), 1995.

[3] Ed. K. Elsener, CERN 98-02, 1998.

[4] T. Bohl, T. Linnecar, E. Shaposhnikova, Phys. Rev. Lett., p.3109, April 1997.

[5] E. Keil, W. Schnell, CERN ISR-TH-RF/69-48, 1969.

[6] D. Boussard, LABII/RF/Int./75-2, CERN, 1975.

[7] K.Y. Ng, FNAL TM 1389, Fermilab, 1986.

[8] E. Shaposhnikova, Proc. EPAC96, p. 1021, 1996.

[9] K. Takayama, D. Arakawa, J. Kishiro, K. Koba, M. Yoshii, Phys. Rev. Lett., p.871, February 1997.